Analyses of Incident Directions of Seismic Rays by the Principal Component Analysis

Itaru Maeda

*Research Center for Earthquake Prediction, Faculty of Science,
Hokkaido University, Sapporo 060, Japan*

(Received October 31, 1981)

Abstract

A new method which determines incident directions of seismic rays from three component data recorded at one seismic station is presented. This method is based on the principal component analysis and has the following characteristics; it conserves phase relation among three components, it may improve S/N ratio in the course of calculations, it can express the variance of the directions of phases composing a P wavelet, and it is adequate to process digitized data semi-automatically.

Applying this method to data obtained by the seismic array system of the Research Center for Earthquake Prediction, Hokkaido University (RCEP), the following results are obtained. (1) The observation system has inherently some causes of error and the amount of error in direction is several degrees. (2) This method gives fairly stable solutions regardless of amplitudes of seismic waves. (3) Underground structure can be deduced by comparing directions obtained by this method and that calculated from locations of earthquakes, and the differences between them are large compared to the errors in (1). (4) Inhomogeneity of the crust may be expressed by the rectilinearity. (5) Local seismic activity can be monitored.

From (3) and (4), it is deduced that, for the Hokkaido region, the structure under the Hidaka mountain range is more inhomogeneous than that of the other regions of Hokkaido and P wave velocity of the land side crust or the upper mantle is lower than that of the ocean side.

1. Introduction

Analyses of the incident directions of seismic rays arriving at an observation point give some information about velocity structures underground and locations of seismic sources (Utsu, 1977). There are not any systematic studies that analyze the incident seismic rays using data obtained by the recent large scale digital network system for seismic observation. In this study

a method suitable for the analysis of digitized three component data is given. We apply systematically the method to the data obtained by the seismic network system of the Research Center for Earthquake Prediction, Hokkaido University (RCEP). Then we discuss the response of the system hardware to this analysis and the small and large scale structure of crust under the Hokkaido region. Detail of the system of RCEP is already reported (Maeda et al., 1978)

2. Theory

Let X_{ij} be three component sampled seismic data where suffix i ($i=1, 2, 3$) indicates the components (U-D, N-S, and E-W), and suffix j means that, at a time t_j, data X_{ij} ($i=1, 2, 3$) are sampled. $X_j=(X_{1j}, X_{2j}, X_{3j})$ can be regarded as a 3-dimensional random variable. We define the expectation value E_i as

$$E_i = \frac{1}{n} \sum_j X_{ij} \tag{1}$$

and the covariance of X_{ij} as

$$C_{il} = \frac{1}{n} \sum_j (X_{ij}-E_i)(X_{lj}-E_l) \tag{2}$$

where n means the total number of the data used. Denoting the covariance matrix composed of C_{ij} as $V=\{C_{ij}\}$, the eigenvectors a and eigenvalues λ are obtained from the eigenvalue equation

$$(V-\lambda 1)\, a = 0 \tag{3}$$

where 1 is the unit matrix.

Let the maximum eigenvalue be denoted as λ_1 and the corresponding eigenvector a_1, and the minimum ones λ_3 and a_3. It is worth noting that the eigenvectors a_i are the axial vectors, that is $(a_i{}^1, a_i{}^2, a_i{}^3)=(-a_i{}^1-a_i{}^2, -a_i{}^3)$, where $a_i{}^k$ ($k=1, 2, 3$) are the components of the eigenvector a_i. For longitudinal waves, the quantity $a_i/|a_i|$ means the incident direction (Montal-Betti et al., 1970) and, for shear waves, it means the polarization direction of the transverse motion in the sense stated above. The propagating direction of the shear wave is determined by $a_3/|a_3|$.

Above interpretations about the quantities $a_i/|a_i|$ and $a_3/|a_3|$ are supported by the theory of principal component analysis (Bolch et al., 1974). In practical applications, a subsidiary condition that a ray propagate upward near an

observation point must be employed to obtain an actual ray direction. This method conserves the phase relation among three components but neglects characteristics of data as a time series. For the latter use we define a quantity α as

$$\alpha = 1 - \lambda_2/\lambda_1 . \tag{4}$$

The meaning of α may be given by the fact that the eigenvalue λ_i is the variance of X in the direction $a_i/|a_i|$, that is, it means the rectilinearity for longitudinal waves and the eccentricity or ellipticity for shear waves.

Next we are concerned with the problem that X is composed of a signal and noise. If an object phase is a S phase, for example, noise consists of P wave coda, reflected waves, tremors, and artificial ground vibrations etc.. superimposed on the S phase. If the frequency band of the signal is apart from that of the noise, the noise can be removed from data using a frequency filter. This is the case, for example, when a short period seismic signal is superimposed on a tremor. On the other hand, when the frequency bands of the signal and noise are superimposed on each other, it is difficult to separate the signal and noise with the frequency filter. In this case, the signal and noise ratio may be improved by the following method.

Let random variable X be composed of a singal X^s and noise X^n, that is,

$$X = X^s + X^n . \tag{5}$$

The expectation values of the signal and noise are defined as before (eq. 1),

$$E_i{}^s = \frac{1}{n} \sum_j X_{ij}{}^s , \qquad E_i{}^n = \frac{1}{n} \sum_j X_{ij}{}^n . \tag{6}$$

Then it may be seen from equations (1), (5), and (6) that the expectation value of the i-the component of X is denoted as

$$E_i = E_i{}^s + E_i{}^n \tag{7}$$

Substituting equations (5) and (7) into (2), we obtain the elements of the covariance matrix as

$$C_{il} = \frac{1}{n} \sum_j (X_{ij}{}^s - E_i{}^s)(X_{lj}{}^s - E_l{}^s) + \frac{1}{n} \sum_j (X_{ij}{}^s - E_i{}^s)(X_{lj}{}^n - E_l{}^n)$$

$$+ \frac{1}{n} \sum_j (X_{ij}{}^n - E_i{}^n)(X_{lj}{}^s - E_l{}^s) + \frac{1}{n} \sum_j (X_{ij}{}^n - E_i{}^n)(X_{lj}{}^n - E_l{}^n)$$

In matrix notation, this may be denoted as

$$V = V^s + V^{sn} + V^{ns} + V^n , \tag{8}$$

where V^s means the covariance of the signal, V^{sn} and V^{ns} mean that of the signal and noise, and V^n means that of the noise. Because the signal and noise are independent of each other in the statistical sense, the covariances of these should be zero. Therefore equation (8) is rewritten as

$$V = V^s + V^n . \tag{9}$$

Because V^n cannot be obtained directly from data, an assumption that noise is stationary in the statistical sense must be made to apply equation (9) in practice. If this assumption holds, we may choose data just before the arrival of the signal as the noise data from which V^n will be constructed. Although the above two assumptions, that is, the signal and noise are independent and the noise is stationary, do not hold strictly in many cases, there may be some cases that these assumptions hold approximately.

3. Application and discussion

Applying the method to various kinds of earthquakes, we explain the responses of the observation system to the analysis, and we discuss the influence of data selection on the results and then discuss local and global velocity structures of the crust under the Hokkaido region.

3.1 System hardware

(1) Setting sensors. It is very difficult to set sensors exactly in the direction intended. But it is possible to correct the results if their directional errors are known. If uncorrected there is a systematic rotation in the resultant directions of the seismic rays. It should not be attributed to anisotropy of the medium.

(2) Relative responses among sensors. It is seldom that the responses of the vertical and horizontal sensors exactly coincide. Table 1 shows the observational 'direction' obtained by analyzing calibration signals of the sensors used at the ERM observatory and the theoretical one which is expected if the responses of three components are exactly equal. The responses of other sensors used in RCEP system are nearly the same as that used at ERM, and have an error of several degrees in direction.

(3) Synchronization of clocks in the system. Some problems arise in a digital seismic telemetering system in which clocks used for data sampling at each seismic station and for multiplexing at the center observatory are not

Table 1 Ideal and actual repsonses of the sensors used at the ERM observatory. U means the result for an up pulse of the calibration signal. D means that for a down pulse. The same number of data are used in these calculations. A large number of data are used to calculate the last values for an up pulse.

		Azimuth	Dip
Theory		225.00	35.2644
Measure	U	222.262	37.971
	D	222.943	37.776
		222.611	37.963
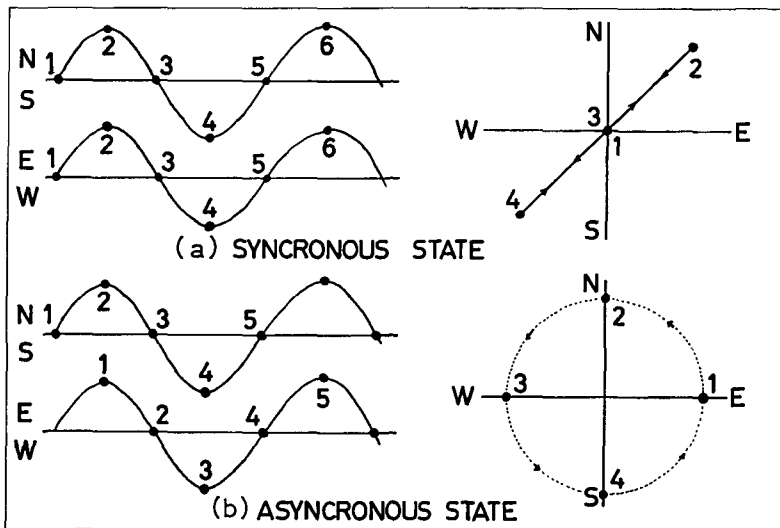
Fig. 1 Schematics of a phenomenon resulting from the difference in clock rate between a sampling station and a recording center.

synchronized. In such a system, a one word lag among channels may happen at the time of multiplexing, which can be illustrated as in Fig. 1–a. As a result of this lag the resultant direction may be disturbed as shown in Fig. 1–b. In the case of figure, the direction of NE-SW and the rectilinearity $\alpha=1$ are obtained if the system is in a synchronous state, but the direction cannot be determined and α equals zero in an asynchronous state with a one word lag. This example is one of the most exreme cases. In many cases, the situation is not so serious that the resultant direction deviates from the true

I. Maeda

Fig. 2　Variation of the dip angle of the Hakodate swarm which were observed at the ESH station and the tidal variation which was recorded at Hakodate.

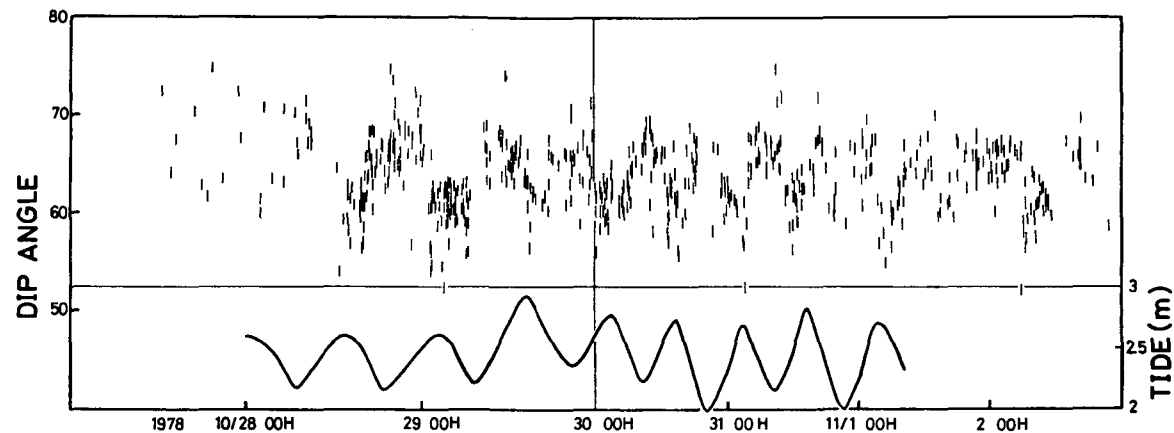one within ten degrees, because the sampling frequency is sufficiently high compared with the dominant frequency of signals. Because the one word lag is caused by the difference in clock rate, the variation in direction may be periodic in time if the clock rates are not equal but constant. This phenomenon was actually observed for the Hakodate micro earthquake swarm which occured from October to November 1978 as shown in Fig. 2. The upper part of the figure shows the variation of the dip angle observed at the ESH station and the lower part shows that of the tide recorded at Hakodate. The variation of the dip angle has a period of about 12 hours and has good correlation with that of the tide. This correlation may be an apparent one and can be explained by the difference of the clock rates of ESH and the center with a difference of 10^{-6}–10^{-7}. If the number of earthquakes per unit time occuring in a region is not sufficiently large, the variation cannot be recognized and it will be considered simply that the results are scattered.

3.2 Deta selection and local structure

(1) Number of data. There is no criterion to determine how many data should be used. The value λ_2/λ_1 becomes small with the limiting value equal to zero, in general, as the number of data used decreases. In the case of P-wavelets, this means the rectilinearity goes to 1. According to our experiences, the direction of an object phase should be determined from data of the first several cycles of the wave motion. When the purpose of the analysis is to deduce a direction of an epicenter, a better result may be obtained by analyzing data over a longer time interval than that of the former case.

Fig. 4 shows the relation between the number of data and the resultant ray directions for a nuclear explosion at Semipalatinsk, USSR on September 1978 recorded at ESH and KMU stations of RCEP. Its seismograms are shown in Fig. 3. The deviation of the resultant direction is a function of the number of data. In the figure, the length of arrows is drawn in proportion to the apparent angle equal to $\pi/2$-dip angle. It is difficult, as can be seen from Fig. 4, to construct a general rule for the number of data to be used. The result at KMU is exceptionally curious and is probably due to the crustal structure under this seismic station. This curious result can be confirmed by the velocity orbit. Fig. 5 shows it for ESH and KMU, which are synthesized from N-S and E-W components. Many phases with different incident directions are clearly distinguished in the orbit of KMU.

(2) Wave length — size of structure. Different frequency components

78 258 11 44 50 COMP= 0 3 6 12 21 25 18 15 9 NDATA=4000 5.0000X
FREQ.= 0.00 99.90 SF 92.3

ESH

HSS
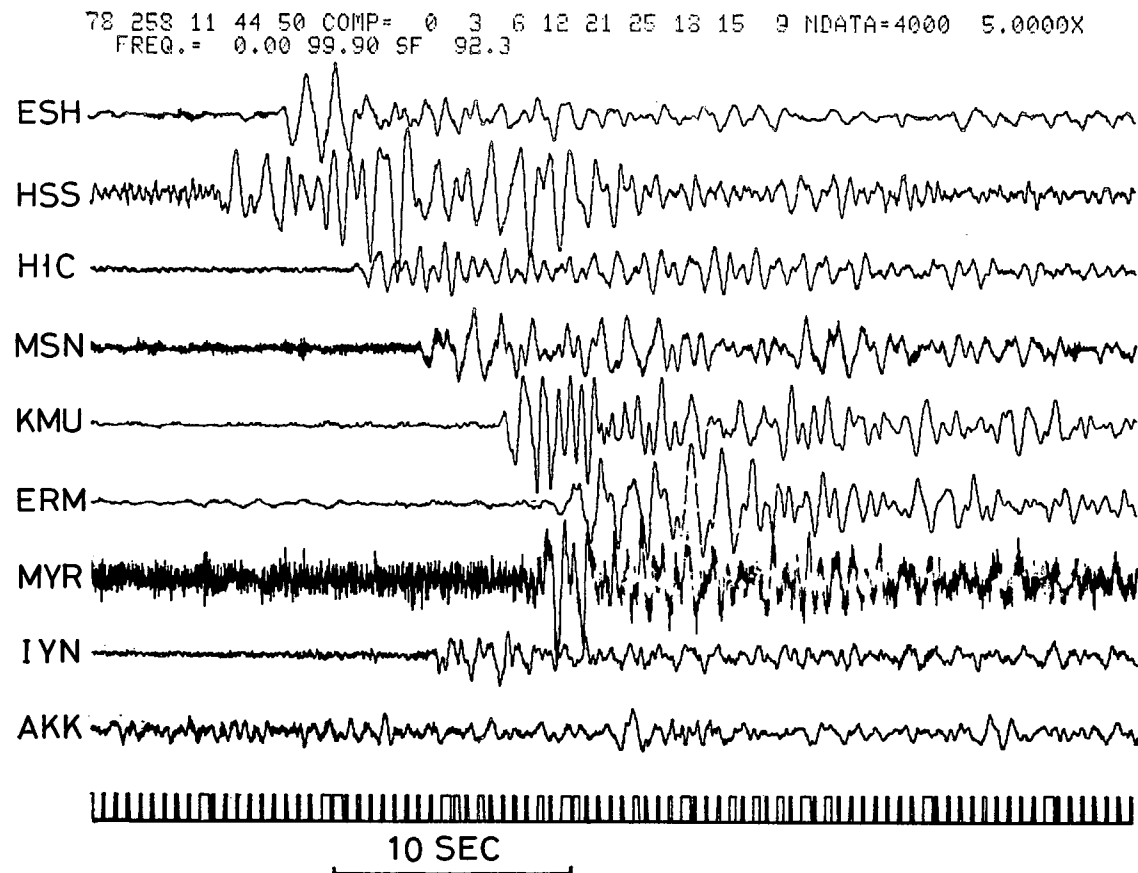
HIC

MSN

KMU

ERM

MYR

IYN

AKK

10 SEC

Fig. 3   Seismograms of the nuclear explosion in the USSR on September 15, 1978.
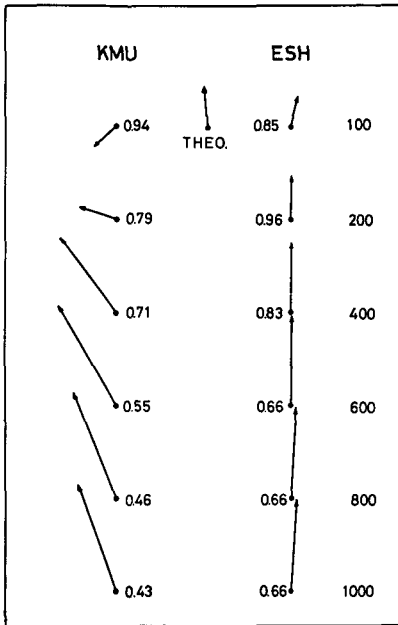
Fig. 4   An example of the relation between the number of data used and the resultant incident direction and the rectilinearity.
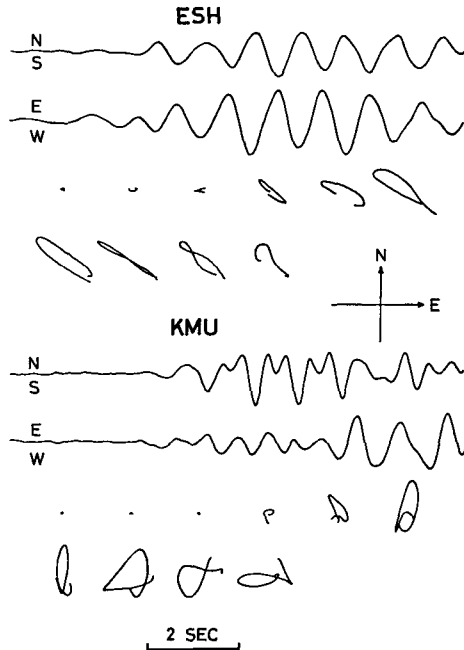
Fig. 5   Velocity orbits synthesized from the data used in Fig. 4.

of a seismic wave may travel different paths. We must take this fact into account if we use a frequency filter. An analysis of the Usu volcanic earthquakes observed at ESH shows the effect of a filter on the obtained incident directions (Fig. 6) The direction calculated from the high frequency component of the signal differs about 60° in azimuth from that of the low frequency one in this case. If we perform systematically this kind of analysis, we may deduce the lateral inhomogeneity of the crust.

   (3) Noise rejection. It is difficult to estimate accurately the effect of noise on the result, because the true seismic signal cannot be known. Here we analyze a case in which stationary noise with rather high frequency is superimposed on a low frequency seismic signal and their amplitudes are not so different. We select data which are obtained at a station such that the calculated directions of rays always approximately coincide with that of theoretical ones which are expected from the locations of earthquakes. The reason that this

case is analyzed is that the noise may be effectively rejected by a frequency filter and an approximate covariance matrix V^n in equation (9) can be constructed using the stationary noise condition. Table 2 shows the results which were calculated by using frequency filters with different frequency bands and V^n for the nuclear explosion in the USSR recorded at MYR on September 1978 (Fig. 3). It can be seen from Fig. 3 that the data satisfy the above conditions. In Table 2, the first row indicates the value obtained from the original data and the second to fourth indicate the values obtained by using the band pass filters with an assigned frequency band. The row assigned NMC indicates the values calculated by using equation (9) in which V^n was constructed from the data just before the P-arrival with the same number of data as that used for P-wavelet. The last row indicates the value calculated from the site of the nuclear explosion by using the table given by Pho and Bahe (1972). The dip angles are all apparent ones except the last.

Table 2   Effects of filters and the noise covariance matrix (NMC)
on noise rejection.

f-range	MYR		
	azimuth	dip	$1-\lambda^2/\lambda^1$
0-30	288	53	0.56
0.5-5.0	302	64	0.83
0.5-2.0	300	66	0.90
0.8-1.2	299	67	0.92
NCM	288	60	0.76
THEO.	305	68	1.00

It can be seen from the table that the results are improved by using the filters and the filter becomes more effective as the band width narrows. The method of NMC is not so effective as the filters, though the rectilinearity and dip angle are somewhat improved. This may be explained by the following reasons. The first is that V^n used in the analysis is not a true one. The second is that the number of data used to construct V^n is not so great that the correlation coefficient between the signal and the noise is not exactly zero.

(4) Amplitude of signal. It is valuable to investigate the stability of solutions by analyzing different earthquakes with the same location of origins. The Usu volcanic earthquakes were analyzed for this propose because these locations are the same within the accuracy of the RCEP telemetering network. Fig. 6 shows the results for earthquakes on November 22, 1977 (EQ1) and
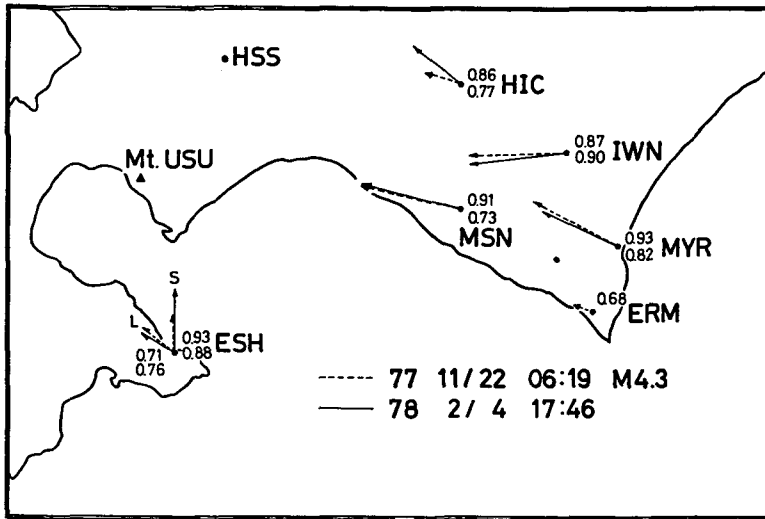
Fig. 6   Ray directions for the large and the small volcanic earthquakes of Mt. Usu.
Assigned values on the right side of the stations are the rectilinearity. The length
of arrows is proportional to $90° -$ dip angle.

February 4, 1978 (EQ2).   These signals have nearly the same dominant
frequency but these amplitudes are very different.   In the figure numerical
values on the right side of the station marks indicate the rectilinearities and
the upper values are for EQ1 and the lower ones are for EQ2.   The somewhat
low rectilinearity obtained for EQ2 is caused by its small amplitude.   Overall
agreement between the two earthquakes means that the present method gives
fairly stable solutions irrespective of signal amplitudes.

3.3   Monitoring of local seismic activity.

We can determine locations of earthquakes using their incident directions
and S-P times, although the accuracy of determination is not good.   We
sometimes need to monitor some local seismic activities which are observed
only at an observation point of a large scale seismic network system.   Motoya
(1980) used the present method to determine the locations of the micro earth-
quake swarm that occurred in the region of Hakodate, and compared them to
the locations obtained by the usual hypocenter calculation using travel times
of P and S waves.   Then he concluded that the present method has the ac-
curacy to monitor local seismic activities.   He used this method extensively to

monitor micro earthquake swarms occurring in the southern part of Oshima peninsula (Motoya, 1981).

3.4 Large scale inhomogeneity

If the velocity structure is laterally homogeneoeus, it is expected that the incident directions of seismic rays arriving at seismic stations of the RCEP network system are nearly the same when we analyze an earthquake whose hypocenter is sufficiently far from Hokkaido.   If the incident directions are not the same, it means that the structure is laterally inhomogeneous and the degree of the inhomogeneity may be expressed by the rectilinearity.

Earthquakes analyzed in this study are listed in Table 3.   Locations and origin times are referred to PDE.   All these earthquakes were recorded with a dominant frequency of about 1 Hz, which was the lower edge of the

Table 3   A list of distant earthquakes analyzed in this study.
The locations are referred to PDE.

N	Y	M	D	H	M	S	LOCATION		Mb	H (Km)
1	76	8	16	14	6	45.9	N32.753	E 104.157	6.1	33
2	76	8	16	16	11	7.3	N 6.262	E 124.023	6.4	33
3	77	9	1	2	59	57.5	N73.376	E 54.581	5.7	0
4	77	11	22	15	56	44.1	S 10.231	E 161.126	5.9	92
5	77	11	23	9	34	58.3	S 31.178	W 66.957	6.0	33
6	77	12	4	11	39	2.8	N48.250	E 146.590	5.1	479
7	78	1	13	20	3	5.2	N45.41	E 150.13	5.3	33
8	78	1	14	3	24	39.1	N34.68	E 139.38	(6.4)	23
9	78	2	7	7	1	39.4	S 0.075	E 124.084	5.9	81
10	78	2	9	21	35	14.9	S 29.81	W177.54	(7.3)	33
11	78	3	4	14	58	8.2	S 4.47	E 152.94	(5.9)	33
12	78	3	7	2	48	46.2	N32.04	E 137.44	6.7	430
13	78	3	15	22	4	40.1	N26.420	E 140.563	6.1	263
14	78	4	12	3	42	3.5	N56.423	E 152.691	6.0	14
15	78	8	3	18	11	15.5	S 26.46	W 70.63	6.7	51
16	78	8	13	20	53	55.0	S 17.70	W178.50	5.4	606
17	78	8	15	12	37	13.4	S 30.42	W178.04	6.3	33
18	78	8	18	18	52	28.0	N59.90	W153.35	5.7	115
19	78	8	23	20	59	2.7	N51.87	E 176.48	5.3	33
20	78	8	29	2	37	6.3	N50.14	E 79.16	5.6	0
21	78	8	31	10	1	16.2	S 5.06	E 151.74	5.3	125
22	78	9	2	1	57	32.4	N24.83	E 121.95	6.3	101
23	78	9	6	11	7	43.9	S 13.20	E 167.13	6.2	200
24	78	9	9	5	41	34.9	N18.59	E 145.50	5.3	204
25	78	9	11	7	40	53.8	N24.94	E 124.86	6.0	33
26	78	9	15	2	36	57.4	N49.85	E 78.69	6.0	0
27	78	9	16	15	35	56.0	N33.21	E 57.35	7.7	33
28	78	9	16	23	38	6.9	S 25.63	W178.14	5.3	200
29	78	9	23	16	32	11.8	S 13.53	E 167.06	5.8	200

Table 4   The azimuth and dip angles and the rectilinearities of the earthquakes listed in Table 2.

	ESH			HIC			MSN			KMU			ERM			MYR			IWN			THEORY	
1	—	—	—	280	71	0.90	284	74	0.90	257	68	0.78	—	—	—	283	61	0.97	261	64	0.90	275	62
2	220	46	0.83	66	85	0.92	158	72	0.89	214	64	0.89	—	—	—	234	61	0.91	214	67	0.97	210	63
3	2	67	0.55	20	57	0.74	338	69	0.75	359	65	0.25	334	73	0.77	245	63	0.65	282	74	0.83	338	64
4	163	54	0.96	106	84	0.89	170	76	0.85	176	62	0.73	209	41	0.43	187	67	0.94	183	75	0.98	158	63
5	32	85	0.80	49	84	0.88	43	71	0.80	340	27	0.65	—	—	—	—	—	—	104	80	0.81	74	90
6	97	81	0.95	46	75	0.98	22	63	0.57	0	54	0.93	28	67	0.83	—	—	—	23	70	0.92	22	*
7	111	77	0.85	86	61	0.85	59	51	0.95	36	57	0.95	85	51	0.96	78	73	0.96	84	65	0.80	58	*
8	204	54	0.30	143	72	0.84	98	57	0.38	275	76	0.85	187	68	0.81	221	54	0.75	220	57	0.87	201	*
9	186	72	0.80	350	73	0.87	138	67	0.33	333	74	0.61	171	71	0.72	236	55	0.91	228	66	0.96	207	65
10	142	67	0.86	57	74	0.72	139	73	0.82	237	61	0.60	147	62	0.42	142	72	0.72	158	68	0.72	146	73
11	183	54	0.96	128	71	0.93	155	72	0.81	211	61	0.61	207	44	0.49	190	67	0.94	171	70	0.98	167	65
12	203	65	0.94	157	76	0.96	232	57	0.91	207	77	0.89	190	59	0.98	243	58	0.80	217	55	0.97	205	*
13	198	69	0.82	151	78	0.84	163	64	0.77	185	69	0.86	179	54	0.90	215	49	0.90	199	58	0.99	188	*
14	109	73	0.55	67	63	0.88	44	62	0.90	274	80	0.76	69	59	0.85	41	73	0.94	29	69	0.91	21	*
15	77	73	0.86	45	71	0.67	—	—	—	28	74	0.57	134	62	0.42	42	83	0.74	322	83	0.87	71	90
16	144	70	0.98	67	77	0.97	128	71	0.86	184	65	0.84	169	65	0.68	187	65	0.91	145	81	0.07	141	71
17	154	69	0.77	22	84	0.78	133	18	0.11	179	54	0.64	204	50	0.55	160	69	0.89	185	78	0.89	147	73
18	78	82	0.85	38	65	0.85	16	62	0.76	24	63	0.78	74	69	0.74	49	78	0.73	12	76	0.87	43	64
19	150	84	0.89	92	82	0.91	40	60	0.88	8	71	0.54	71	66	0.79	—	—	—	37	69	0.96	56	59
20	304	69	0.92	328	68	0.82	44	79	0.73	320	63	0.69	228	59	0.76	305	68	0.92	271	58	0.81	303	64
21	186	48	0.89	328	86	0.91	150	64	0.82	197	44	0.58	233	60	0.81	231	57	0.88	217	64	0.95	168	66
22	246	49	0.87	151	83	0.63	201	77	0.84	215	69	0.85	223	63	0.60	250	54	0.94	231	61	0.86	231	60
23	144	61	0.82	62	85	0.76	32	49	0.66	—	—	—	130	88	0.66	184	65	0.81	166	74	0.96	153	68
24	149	73	0.38	136	82	0.75	87	64	0.77	283	83	0.83	142	57	0.41	201	54	0.79	177	67	0.88	174	60
25	238	67	0.79	121	48	0.65	295	70	0.44	230	74	0.76	214	55	0.74	242	43	0.87	217	59	0.87	226	58
26	301	52	0.83	38	75	0.83	34	70	0.81	321	68	0.80	217	60	0.73	297	60	0.82	265	57	0.74	303	64
27	296	63	0.81	343	71	0.66	348	79	0.90	196	46	0.35	225	60	0.71	319	69	0.84	301	70	0.67	293	69
28	111	74	0.83	78	73	0.91	116	84	0.77	130	56	0.78	182	45	0.80	—	—	—	119	80	0.85	145	72
29	159	66	0.86	39	84	0.97	48	61	0.68	201	68	0.71	174	79	0.56	182	71	0.93	192	76	0.98	153	68
M	22		0.82	65		0.85	41		0.73	42		0.73	34		0.68	26		0.85	23		0.89		

pass band of RCEP system. Results for P wavelet are listed in Table 4. In the table theoretical values are calculated using the locations listed in Table 3 and the travel time table by Pho et al. (1972). The dip angles are measured from the horizontal. In the calculation of equation (3), the conditions stated in 3.2 were taken into account. Therefore the number of data and the pass band of the filters used are different in each case.

The average values of the rectilinearity of MSN, KMU, ERM, and HIC are lower than that of the other stations. Although these values are not very wrong due to the above conditions, the difference between the two groups of stations becomes large if the same number of data and the same filter are used in the analyses. Deviations in azimuth from the theoretical values for the stations located in the southwest rim of the Hidaka mountain range are relatively large compared with that for the other stations. These mean that the crustal structure under this region is more inhomogeneous than that of the other region. The dimension or the correlation length of inhomogeneity which affects the analyzed seismic waves is on the order of 10 Km. At these stations, remarkable phases other than P and S phases are frequently observed (Shimizu and Maeda, 1979, 1980). These phases are explained by the existence of an inclined boundary plane at which seismic
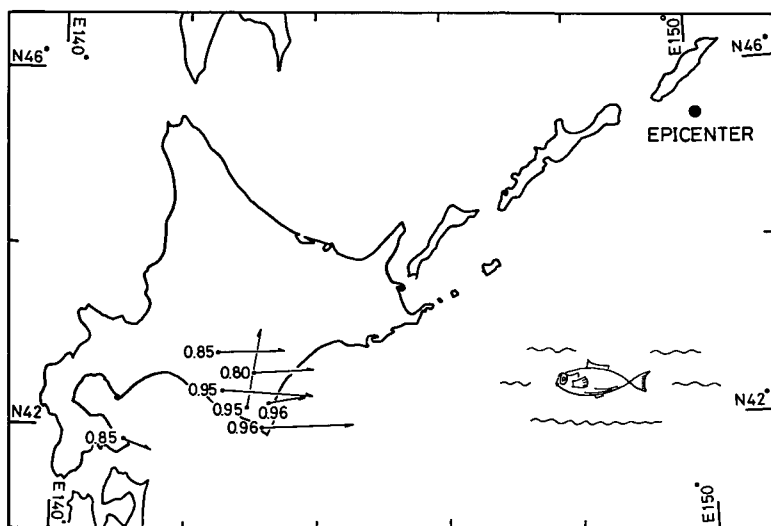

Fig. 7   Calculated directions for off Etorofu earthquake on January 14, 1978, whose epicenter is indicated by ●.   Arrows point to not the epicenter but the ocean side.

waves are reflected.   This supports the above result.

It is also seen in the table that the average dip angle obtained at HIC is relatively large compared with that of the other stations.   This means that the surface layer is relatively thick or its velocity is relatively low compared with that of the other stations.

In Fig. 7 the incident directions and the epicenter of the earthquake on January 14, 1978 off Etorohu island are indicated.   The length of arrows is drawn in proportion to the apparent dip angle.   It can be seen from the figure that the seismic waves arrive at the stations except KMU not from the direction expected from the epicenter but from the ocean side.   This means that the P wave velocity of the landside crust or the upper mantle is lower than that of the ocean side.

4. Conclusion

A method which gives incident directions of seismic waves from three component seismograms is described in section 2.   This method is adequate to process digital data semiautomatically.   Its characteristics are that it conserves the phase relation among three components and can remove noise to some degree.   Some of causes of error---error means deviation of a calculated direction from that expected from a location of an earthquake---in the resultant directions are inherent to the observation system (*3.1*).   Some of these can be removed provided that we examine the characteristics of the system and correct the results.   But some other (*3.1*--(3)) can not be removed.   The other causes of error are from the structure of the crust or the mantle.   Then we obtained qualitative results about inhomogeneity of the crust.

The present method is useful to monitor local micro seismic activities.

References

Bolch, B.W. and C.J. Huang, 1974.   Multivariate statistical methods for business and economics.   Prentice-Hall, London. 286 pp.

Maeda, I., Y. Motoya, and S. Suzuki, 1978.   On the telemetered data recording and processing system for earthquakes and earthstrains at Hokkaido university (in Japanese). Zisin, **31**, 401–413.

Montalbetti, J.F. and E.R. Kanasewich, 1970.   Enhancement of teleseismic body phases with a polarization filter, Geophys. J. astr. Soc., **21**, 119–129.

Motoya, Y., 1980. private communication

Motoya, Y., 1981.   On the earthquake sequences in the Oshima peninsula, southern part of Hokkaido (in Japanese), Zisin, **34**, 105–121.

Pho, H.T. and L. Behe, 1972. Extended distances and angles of incidence of P waves,
      Bull. Seism. Soc. Amer., **62**, 885–902.
Shimizu, N. and I. Maeda, 1979. Analysis of remarkable phases for shallow earthquakes
      occuring under the Hidaka mountain region (in Japanese), Zisin, **32** 142–163.
Shimizu, N. and I. Maeda, 1980. Analysis of seismic waves with remarkable phases
      observed at station KMU (in Japanese), Zisin, **33**, 141–155.
Utsu, T., 1977. Seismology (in Japanese), Kyoritu, Tokyo 286 pp.